Mitigation of Geomagnetically Induced Currents Using Corrective Line Switching

Maryam Kazerooni, *Student Member, IEEE*, Hao Zhu, *Member, IEEE*, and Thomas J. Overbye, *Fellow, IEEE*

***Abstract*—This paper considers line switching as a remedial action to mitigate the geomagnetically induced currents (GICs) in large-scale power systems. The algorithm uses linear sensitivity analysis to find the best switching strategy which minimizes the GIC-saturated reactive power loss. Furthermore, the coupling between the ac power flow solution and the GIC flows is modeled and heuristic strategies are designed to maintain the system security measures in terms of both GICs and ac power flow. Finally, the computational complexity of the algorithm is analyzed for large-system implementations. To reduce the complexity, the critical lines are identified through the sensitivity analysis and the calculations are performed only on the reduced system. The effectiveness of the proposed algorithm is demonstrated through numerical results using a small 20-bus test case as well as large power systems.**

***Index Terms*—Geomagnetically induced currents (GICs), line switching, transformer reactive power loss, transmission system analysis.**

I. Introduction

SOLAR coronal holes and coronal mass ejections can disturb the Earth's geomagnetic field. These geomagnetic disturbances (GMD) in turn induce electric fields which drive low frequency currents in the transmission lines. These geomagnetically induced currents (GICs) can cause increased harmonic currents and reactive power losses by causing transformers half-cycle saturation. This may cause voltage instability by a combination of two means. First, the increased transformer reactive power losses may lead directly to voltage instability. Second, the harmonic currents might cause relay misoperation and unintended disconnection of the reactive power providers such as static VAR compensators [1]–[4].

The negative impacts of GMDs have motivated the US government to improve their understanding of GMDs and prepare the bulk power system for potential events [5], [6]. Several techniques have been investigated in the literature to mitigate GMDs [7], [8]. One technique is to install GIC blocking devices with the capacitive circuits at the transformer neutral. If placed at proper locations, this technique can reduce the GIC-saturated reactive power loss [9], [10]. Installing a capacitor in the neutral may compromise the ground fault detection system or cause insulation hazards and safety risks. Possible solutions to reduce such risks are using parallel resistors or spark gaps, vacuum switching or interrupting the protection circuit [11], [12]. The tradeoff among these solutions envolves complexity, bulkiness and deployment cost. Series capacitors [10], polarizing cells [13], and neutral linear resistance [13], [14] are other types of blocking devices investigated in literature for GMD mitigation.

Line switching has been studied as an effective control strategy to improve power system reliability [15]–[18]. Line outage distribution factors (LODFs) are utilized in [19] to rank the candidate switching actions. Similar types of sensitivity factors have been employed in [20] and [16] to determine the best switching actions. In general, line switching can modify the network-wide flows so that the overloads and voltage violations are relieved. Using the same concept, the GIC flows could be redirected through line switching to reduce the negative impacts. To the best of our knowledge, GMD mitigation through topology control has not been investigated in literature so far.

The existing GIC mitigation programs focus only on the dc analysis of the system and reducing the GIC flows. However, the ac power flow solution is coupled with the GIC flows and it is desired that the mitigation framework integrates some aspects of the ac analysis along with the already existing dc ones. This is especially important when line switching or series capacitors are considered as the control action. Line switching changes the ac flows and if not performed correctly, may cause overloads and voltage violations. An effective GMD mitigation should properly model the effect of GICs on the ac power flow solution and develop a strategy that provides sufficient security measures in terms of both GIC flows and ac analysis.

In this paper, topology control is considered as a remedial action to protect the network from GMDs. Similar to the conventional LODFs, transformer LODFs (TLODFs) are defined as the sensitivity of the transformer GIC-saturated reactive power loss to line outages. An iterative algorithm is developed to find the best line switching strategy which minimizes the total GIC-saturated loss based on TLODFs. Opening a line changes the topology and the algorithm requires updating the TLODFs in each iteration. This is computationally expensive and may not be practical for large-systems implementations. To reduce the complexity, the critical lines are identified based on the initial TLODFs and the line selection strategy is applied to only those lines. Finally, the coupling between the ac power flow solution

Manuscript received December 14, 2016; revised May 22, 2017 and August 14, 2017; accepted August 28, 2017. Date of publication September 22, 2017; date of current version April 17, 2018. This work was supported by the National Science Foundation through "EAR-1520864: Hazards SEES: Improved prediction of geomagnetic disturbances, geomagnetically induced currents, and their impacts on power distribution systems" Paper no. TPWRS-01869-2016. *(Corresponding author: Maryam Kazerooni.)*

The authors are with the Department of Electrical and Computer Engineering, University of Illinois at Urbana-Champaign, Urbana, IL 61801 USA (e-mail: kazeron2@illinois.edu; haozhu@illinois.edu; overbye@illinois.edu).

Color versions of one or more of the figures in this paper are available online at http://ieeexplore.ieee.org.

Digital Object Identifier 10.1109/TPWRS.2017.2753840

and the GIC flows are modeled and proper heuristics are developed to maintain sufficient ac-related security measures. The effectiveness of the algorithm is demonstrated through numerical results using a small 20-bus test case, a medium-size 150-bus system, and finally a large 2000-bus case.

The paper is organized as follows: The GIC model is introduced in Section II and solving power flow including GICs is described in Section III. The proposed line selection algorithm is presented in Section IV. Section V demonstrates the proposed technique through numerical results. Section VI presents a conclusion and direction for future work.

II. GIC MATRIX

To calculate the voltage potential induced on the transmission line, the E-field is integrated over the length of the line. Assuming uniform E-field, the DC voltage on the line between bus n and m is expressed in:

$$V_{nm} = E^N L^N_{nm} + E^E L^E_{nm} \tag{1}$$

where L^N_{nm} and L^E_{nm} denote the northward and eastward distances of the line (n, m); and E^N and E^E are the northward and eastward E-fields, respectively. The induced voltages are converted to the dc current injections through Norton Equivalent, and the total current injections are derived from Kirchhoff's current law (KCL) [3], [9]. The vector of current injections is obtained by putting all the current injections together as given by $\mathbf{I} = \mathbf{HE}$ where $\mathbf{H}$ depends on the length, orientation, and resistance of the lines [21].

To obtain the GIC flows, stack the dc voltage V_n at any bus or substation neutral in $\mathbf{V} := [V_1, \ldots, V_N]^T$, which follows the dc power flow model as

$$\mathbf{V} = \mathbf{G}^{-1}\mathbf{I} = \mathbf{G}^{-1}\mathbf{HE} \tag{2}$$

where matrix $\mathbf{G}$ is similar to the bus admittance matrix except that it only captures the conductance values and is modified to include the substation grounding resistances. The size of the matrix is $(N + S) \times (N + S)$ where S is the number of substations and the additional rows/columns model the grounding resistances. Note that V_n is the dc node voltage, different from the induced line voltage V_{nm}. The GIC flow between any two nodes is given by

$$I^T_{nm} = g_{nm}(V_n - V_m) \tag{3}$$

where g_{nm} is the (n, m)-th entry of the matrix $\mathbf{G}$.

A. GIC-Saturated Reactive Power Loss

The GIC passing through the transformer increases its reactive power loss. A simplified model is presented in [4] which relates the additional GIC-saturated reactive power loss (GRPL) to the effective GICs as expressed in:

$$Q^{GIC} = KV^{pu} I^{GIC} \tag{4}$$

where Q^{GIC} is the GRPL. K is the transformer loss coefficient which mostly depends on the core type, e.g., single phase, three-legged three phase and five-legged three phase. This parameter may be calculated by simplifiying the tranformer magnetizing curve into linear segments and determing the slope and knee point of each segment [22]. V^{pu} is the ac voltage magnitude of the transformer's high-voltage side. Note that obtaining this value requires the ac power flow solution. The voltage profile of the base case or a flat voltage profile may be used instead to decouple the GIC-saturated loss from the ac analysis and simplify the calculations. Any reference to losses throughout the paper indicates the GIC-saturated reactive power loss.

I^{GIC} is the effective GIC and is calculated based on the transformer type and winding configuration. For a grounded wye-delta transformer, I^{GIC} is simply the current in the grounded coil. For transformers with multiple grounded windings (-autotransformers), the effective current is a function of the current in both coils as expressed in [23]:

$$I^{GIC} = \frac{aI_H + I_L}{\alpha} \tag{5}$$

where I_H and I_L are respectively the per phase dc current passing through the high side winding (-series winding) and low side winding (-common winding) and α is the transformer turn ratio. Calculating I_H and I_L from (3), the effective current at transformer t is given by:

$$I^{GIC}_t = g_{sh}(V_h - V_s) + \frac{1}{\alpha} g_{sl}(V_l - V_s) \tag{6}$$

where h and l are the high and low side bus nodes for transformer t, and s is its substation node. Concatenating (6) across all transformers gives rise to:

$$\mathbf{I}^{GIC} = \mathbf{\Phi V} = \mathbf{\Phi G}^{-1}\mathbf{HE} \tag{7}$$

where $\mathbf{\Phi}$ is a $T \times (N + S)$ matrix with the (t, m)-th entry given by

$$\Phi_{tm} := \begin{cases} g_{sm}, & \text{if } m = h \\ \alpha g_{sm}, & \text{if } m = l \\ -g_{sh} - \alpha g_{sl}, & \text{if } m = s \\ 0, & \text{otherwise.} \end{cases} \tag{8}$$

and T is the number of transformers.

B. Effect of Line Switching on GIC Flows

Next, the effect of opening a line on the GIC flows is studied. Opening line (n, m) modifies the $\mathbf{G}$ matrix by deducting the terms related to the disconnected pairs:

$$\mathbf{G} \leftarrow \mathbf{G} - g_{nm} e_{nm} e^T_{nm} \tag{9}$$

where vector e_{nm} of length N has all zero entries except for the n-th and m-th being +1 and -1, respectively. Similarly, the $\mathbf{H}$ matrix is modified by

$$\mathbf{H} \leftarrow \mathbf{H} - e_{nm}[L^N_{nm}, L^E_{nm}] \tag{10}$$

Opening a line does not affect the $\mathbf{\Phi}$ matrix. Opening multiple lines requires updating $\mathbf{G}$ and $\mathbf{H}$ successively for each opened line.

III. POWER FLOW SOLUTION INCLUDING GICS

To solve power flow including the GICs, the GIC-saturated reactive power loss of each transformer is modeled as a constant

current source. Adding these current sources changes the reactive power injections at the high voltage side of the transformers by:

$$Q_i \leftarrow Q_i - KV_i^{pu} I_i^{GIC} \tag{11}$$

where Q_i is the reactive power injection at bus i. The power balance equations are nonlinear and the most common technique for solving them is Newton-Raphson solution. This technique uses the first order Taylor series to linearize the power balance equations as expressed in:

$$\begin{bmatrix} \Delta\theta \\ \Delta|\mathbf{V}| \end{bmatrix} = -\mathbf{J}^{-1} \begin{bmatrix} \Delta\mathbf{P} \\ \Delta\mathbf{Q} \end{bmatrix} \tag{12}$$

where $\Delta\mathbf{P}$ (-$\Delta\mathbf{Q}$) is the vector containing all the real (-reactive) power imbalances and $\mathbf{J}$ is Jacobian matrix defined as:

$$\mathbf{J} = \begin{bmatrix} \dfrac{\partial\Delta\mathbf{P}}{\partial\Delta\theta} & \dfrac{\partial\Delta\mathbf{P}}{\partial\Delta|\mathbf{V}|} \\ \dfrac{\partial\Delta\mathbf{Q}}{\partial\Delta\theta} & \dfrac{\partial\Delta\mathbf{Q}}{\partial\Delta|\mathbf{V}|} \end{bmatrix} \tag{13}$$

The algorithm starts with an initial guess, uses (12) to update the states in each iteration and continues the process until the power mismatches are smaller than a threshold. Adding the GIC-related constant current sources modifies the entries of the Jacobian that correspond to the partial derivative of the reactive power to voltage magnitudes of the same bus:

$$\frac{\partial\Delta Q_i}{\partial\Delta|V_i|} \leftarrow \frac{\partial\Delta Q_i}{\partial\Delta|V_i|} - KI_i^{GIC} \tag{14}$$

The other entries of the Jacobian matrix stay unchanged.

IV. Iterative Line Switching Algorithm

The transformer heating during GMDs is caused by a combination of increased GIC-saturated reactive power loss and harmonics. Both factors are directly related to the effective GICs on the transformer. In this section, an iterative algorithm is proposed which reduces the transformer heating through minimizing the GIC-saturated reactive power loss. The principles of the algorithm is presented in the following, techniques to reduce the computational complexity are designed in Section IV-A and heuristic strategies are incorporated in Section IV-B to provide sufficient ac-related security measures.

The transformer LODF (TLODF) can be expressed as:

$$TLODF = [s_{ij}] = \left[Q_i^{GIC,(j)} - Q_i^{GIC,(0)}\right], \quad i \in T,\ j \in L \tag{15}$$

where s_{ij} is the variation of GIC-saturated loss at transformer i caused by opening line j, $Q_i^{GIC,(j)}$ is the GIC-saturated loss at transformer i when line j is opened and $Q_i^{GIC,(0)}$ is the initial loss. An analytical technique may be developed to derive TLODFs as a function of the network parameters. Alternatively, one can follow the sensitivity definition to calculate the TLODFs as described in Algorithm 1. L in the algorithm is the number of lines.

Algorithm 1: Determining the TLODF.

procedure Determining the TLODF
  Calculate the initial GIC-saturated loss at each transformer, $\mathbf{Q}^{GIC,(0)}$
  for $1 \le n \le L$ **do**
    Open line n
    Calculate the GIC-saturated loss at each transformer, $\mathbf{Q}^{GIC,(n)}$
    Calculate the n^{th} column of the TLODF matrix by $\mathbf{Q}^{GIC,(n)} - \mathbf{Q}^{GIC,(0)}$
    Close line n
  end for
end procedure

Algorithm 2: Iterative Line Selection.

procedure Selecting Best Lines to Open
  for $1 \le m \le M$ **do**
    Calculate TLODFs
    Calculate Q^T from TLODF
    Find the line with lowest Q^T and open that line.
  end for
end procedure

TLODFs are used to identify the best line switching strategy that minimizes the GIC-saturated loss. The total loss reduced from opening a line is obtained by taking the sum of TLODF matrix along the corresponding column. Let $Q^T = Sum(TLODF, 2)$ be the sum of the TLODF matrix along the columns. The best lines are obtained by sorting Q^T in descending order and selecting the lines with the lowest Q^T values.

Similar to LODFs, TLODFs consider single line outages. The TLODF for multiple-line outages is not equal to the sum of the single-line TLODFs of the corresponding lines. The notion of generalized LODF was introduced in [24] which considers multiple-line LODFs. A similar concept may be considered for TLODF and analytical techniques can be developed to calculate multiple-line TLODFs. A rather simple approach for calculating TLODFs under multiple-line outages is to consecutively open one line and calculate the single-line TLODFs for the new system until all the desired lines are opened. The line switching algorithm can thus be improved using a similar approach. First, the TLODF is calculated and the best line to be opened is selected accordingly. Next, the TLODF matrix is calculated for the new system and the second line to be opened is selected. This process is repeated until the number of opened lines reaches a user-defined threshold, M. This technique is presented in Algorithm 2.

A. Reducing the Computational Complexity

The computational complexity of the proposed algorithm is $\mathcal{O}(LMT)$ where L is the number of lines, M is the maximum number of lines that can be opened and T is the computation time for solving for GIC flows. The number of lines for a power grid is typically slightly larger than the number of buses. Solving GIC

Algorithm 3: Fast Iterative Line Selection.

procedure Selecting Best Lines to Open
  Initialize the number of opened lines, m to zero.
  while $m \leq M$ **do**
    Calculate full TLODFs.
    Calculate Q^T from TLODF.
    Find the critical lines from Q^T.
    for $1 \leq c < U$**do**
      Update TLODFs for critical lines.
      Update Q^T of critical lines.
      Find the line with lowest Q^T and open it.
      $m = m + 1$.
      if $m \leq M$ **then**
        Break
      end if
    end for
  end while
end procedure

Algorithm 4: Power Flow Solution Check.

procedure Find the Line with Power Flow Solution
  for $1 \leq c <$ C**do**
    Open Line c in the sorted list.
    Calculate the Y-bus for the new System.
    if new Y-bus is full rank**then**
      Return line c.
    end if
    Close line c.
  end for
end procedure

flows requires calculating the inverse of $\mathbf{G}$ and then multiplying it by $\mathbf{\Phi}$. $\mathbf{G}$ is a sparse matrix roughly in the order of $O(N^2)$ and the computation time of taking its inverse is $\mathcal{O}(N^{2.2})$ [25]. $\mathbf{\Phi}$ is a sparse matrix of roughly the same order and multiplying it by $\mathbf{G}^{-1}$ requires $\mathcal{O}(N^{2+\mathcal{O}(1)})$ [26].

To reduce the running time, first, the TLODF matrix is calculated and Q^T is calculated for each line by taking the sum of the TLODF matrix over its columns. The first C lines in the sorted list are selected as critical lines and are investigated for further analysis. C is a user-defined parameter which controls the complexity. After selecting the critical lines, the iterative line selection algorithm is applied to only these lines; i.e., the TLODFs are calculated for only the critical lines and the optimal lines are obtained based on the Q^T values. The critical lines may be updated after each U iterations by recalculating the full TLODF matrix. U is again a user-defined parameter which controls the computation time. Some insights on how to select suitable C and U values are presented later through simulation. Details of the fast line selection algorithm are presented in Algorithm 3.

Parallel computing may be used to further reduce the running time. The columns of the TLODF matrix can be calculated in parallel which reduces the running time by the order of the number of processors. Another approach to improve the computational complexity is to take advantage of the small network modification in computing the inverse of G. Instead of computing the full $\mathbf{G}^{-1}$ each time a line is opened, it could be calculated just once for the base case and then be derived from the base case through rank-1 update in $\mathcal{O}(N)$ or $\mathcal{O}(N^2)$ computations. The switching design procedure would probably be performed off-line, and therefore the computational complexity is not very critical. However, it may be desired to perform the analysis in real-time as the switching strategy depends on the state of the system, e.g., induced E-field and ac line flows (dependency on the ac flows will be explained in the next subsection).

B. Incorporating AC Analysis Into the Algorithm

Opening a line changes the structure of the Jacobian matrix and the new system may not have a power flow solution. The line selection algorithm should guarantee that the switching strategy provides a power flow solution. One possible procedure to ensure this is as follows: The algorithm starts with the fist line in the sorted list. The candidate line is opened and the Y-bus of the new system is calculated. If the new Y-bus is full rank, the candidate line is selected. If not, it is discarded and the second line in the sorted list is considered as the new candidate. The process is continued until a line that provides a full-rank Y-bus is found as detailed in Algorithm 4. This process is performed instead of step five in Algorithm 2 or step 10 in Algorithm 3. Note that calculating the new Y-bus after opening a line is not computationally expensive as it can be derived from the initial Y-bus in negligible computational time.

Factors other than TLODFs may be used as a criterion for selecting the best lines. The power system experiences reactive power shortage during GMDs and reducing the GIC reactive loss is desired. However, opening a line changes the AC flows in the system and may compromise the system security. Hence, a meaningful line selection algorithm should consider some aspects of the ac analysis along with the already existing GIC related criterion (GIC-saturated loss). Motivated by this, the AC line flow may be considered as an additional criterion for selecting the best lines:

$$F_i = \frac{Q_i^T}{\bar{P}_i} \tag{16}$$

where $\bar{P}_i$ is the flow on line i. F is calculated for all the lines and the line with the highest absolute value of F is selected in each iteration. This criterion selects the line that reduces the GIC-saturated loss more and also has lower AC flow on it. Note that the ac flows change at each iteration and hence ac power flow needs to be solved to update them. This adds complexity to the algorithm and increases the running time. The ac flows may be updated after several iterations as opposed to every single iteration to reduce the running time associated with solving power flow. Moreover, the algorithm may be performed offline as part of the system planning in which case the running time would not be a constraint.

A voltage violation index may be defined to speculatively evaluate the resultant security of the system after executing the line switching scheme. The total amount of voltage violation is

calculated by:

$$V_i^{\min} \le V_i \le V_i^{\max}$$
$$SV = \sum_i \max\{0, V_i - V_i^{\max}, V_i^{\min} - V_i\} \qquad (17)$$

where V_i is the per unit voltage magnitude at bus i. $V_i^{\min} = 0.95\ pu$ and $V_i^{\max} = 1.05\ pu$ are typically considered in reliability studies and hence are used in this paper.

C. Line Switching Strategy Through Exhaustive Search

The iterative line switching algorithm is computationally efficient and scalable to larger systems; however, its solution is not optimal. The problem of finding multiple best lines is simplified to finding the single best line in each iteration. This provides the local optimum and not necessarily the global one. Moreover, the procedure to guarantee the power flow solution is naive and the algorithm may fail to find the existing feasible actions that can provide power flow solutions. Examples of such corner cases will be shown later. For smaller systems, alternative approaches may be used which are more computationally expensive, yet provide a better solution. A greedy algorithm applicable to small systems is described below:

Let M be the maximum number of lines that can be opened and L be the number of lines. All distinct ways of selecting M lines from L lines are considered, i.e., $\binom{L}{M}$ combinations. For each candidate action, the selected lines are opened, the GICs for the new system are calculated and the resulting loss is obtained. The combinations are sorted based on their associated losses, and the action which provides the lowest loss is chosen as the best action. For a large system, the number of possible combinations is huge and performing exhaustive search is not practical. To address this, the search can be narrowed down by finding the critical lines and performing the exhaustive search on only those lines. The critical lines are identified based on the TLODFs and the Q^T values. This reduces the running time from $\binom{L}{M}$ to $\binom{L}{C}$ where C is the number of critical lines.

V. Numerical Results

In this section, the algorithm is applied to systems of varying sizes and its performance is evaluated through numerical results.

A. 20-Bus System

First, the 20-bus system in [27] is investigated with the one-line diagram shown in Fig. 1. An electric field with the magnitude of 8V/km and the orientation of 124° N is enforced to the system. This orientation results in the largest GICs for the system and hence is considered for the analysis. The line selection algorithm is utilized to minimize the GIC-saturated loss. A combination of TLODFs and ac line flows is considered as the selection criteria as proposed in (16). The selected lines in each iteration and the resulting total loss are presented in Table I. The algorithm is terminated after the third step since opening any of the remaining lines results in an ill-conditioned Jacobian and no power flow solution. The running time of the algorithm is 0.29 seconds and it includes the ac power flow solution at each iteration. The computations are performed on a Dell XPS 8900 system with Intel core i7, 16GB RAM.

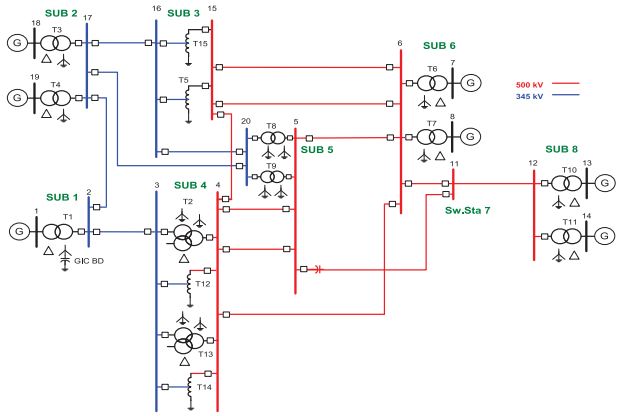

Fig. 1. One-line diagram of the 20-bus system in [27].

TABLE I
Line Switching Solutions Obtained From the Iterative Algorithm for the 20-Bus System

Order	Opened Line (To Bus, From Bus)	Total Loss
0	–	19.68
1	(4,5)-First line	18.16
2	(4,5)-Second line	15.24
3	(4,6)	12.34

Running Time: 0.29 s

TABLE II
Line Switching Solutions Obtained From the Exhaustive Search for the 20-Bus System

Number of Opened Lines	Action Number	Opened Line (To Bus, From Bus)	Total Loss (pu)	Running Time (s)
2	1	(6,15), (6,15)	13.39	1.61
	2*	(4,5), (4,5)	15.24	
3	1	(4,5), (6,15), (6,15)	12.10	8.49
	2*	(4,5), (4,5), (4,6)	12.34	
4	1	(4,5), (4,6), (6,15), (17,20)	11.56	30.43
5	1	(4,5), (4,6), (6,15), (16,20), (17,20)	10.66	78.94

Next, the iterative algorithm is compared with the exhaustive search. Table II presents the best actions obtained from the exhaustive search when the number of opened lines, M, changes from two to five. Power flow is solved for all the possible combinations in the exhaustive search and the ones with non-promising ac solutions are ignored. The running times presented in the table includes the running time of solving the power flows. For $M = 2$ and $M = 3$, the second best action found by the exhaustive search is the same as the one obtained from the iterative algorithm (shown by * in the table). This indicates that the solution from the iterative algorithm is very close to the optimal solution. For $M = 4$ and $M = 5$, the exhaustive search still manages to find feasible solutions, unlike the iterative algorithm that terminates at the third iteration. This shows that the procedure to find feasible actions with power flow solutions is naive and there might be corner cases that the iterative algorithm fails to find.

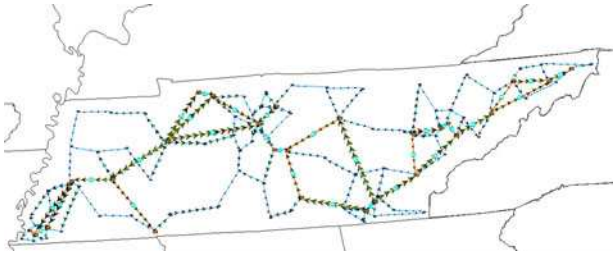

Fig. 2. One-line diagram of the150-bus synthetic system; the green lines are 500 kV and the blue lines are 230 kV.

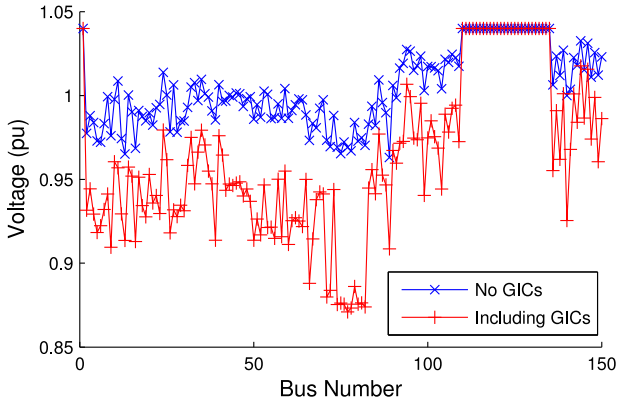

Fig. 3. The effect of GICs on the voltage profile of the 150-bus system.

B. 150-Bus Synthetic System

The next system to study is the medium-size 150-bus synthetic system in [28], [29] with the one-line diagram illustrated in Fig. 2. The green lines in the one-line diagram are 500 kV and the blue lines are 230 kV. This case is entirely synthetic, built from the public load/generation data of the Tennessee region and a statistical analysis of real power systems.

An electric field with 8v/km magnitude and 26° N orientation is enforced to the system. Again, the motivation for choosing this orientation is that it provides the highest GICs. The GIC flow is solved and the resulting GIC-saturated loss is calculated. Fig. 3 shows the effect of GICs on the voltage profile. The system experiences reactive power shortage due to the GIC-saturated loss and the voltage at most of the PQ buses falls below the permissible value, i.e., 0.95 pu.

The line selection algorithm is utilized to minimize the loss. Fig. 4 illustrates the performance of the algorithm using two approaches: 1) using TLODFs as the criterion to select the best line, 2) using a combination of TLODFs and ac line flows as proposed in (16). Both approaches reduce the total loss as more lines are opened. The total loss is lower when only TLODFs are considered. However, the algorithm terminates at the seventh iteration since no other action with power flow solution can be found beyond that point. Including the ac line flows in the algorithm results in larger loss in each iteration, yet the algorithm can proceed up to the 21st iteration while still providing a feasible solution. The final solution obtained at the last iteration of this approach has a lower loss than the one obtained from the last step of the first approach which includes only TLODFs.

The violation index in (17) is used to compare the security of the system under the two scenarios as shows in Fig. 5. The

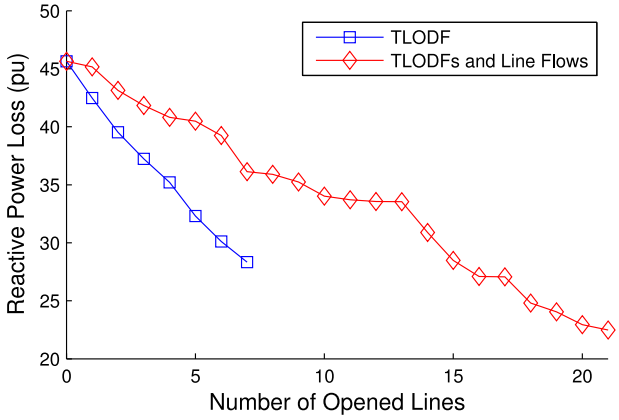

Fig. 4. Total GIC-saturated reactive power loss in terms of the number of opened lines using the proposed line switching algorithm.

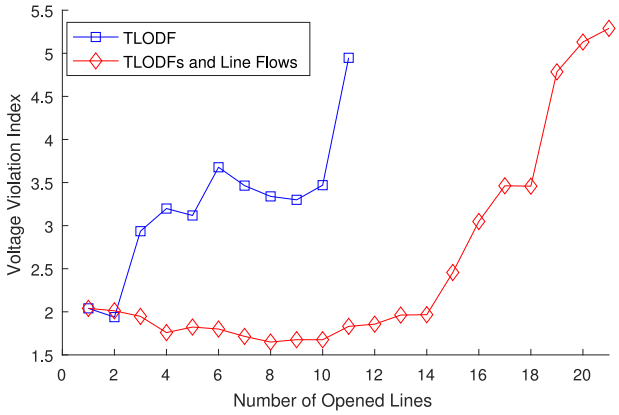

Fig. 5. The impact of incorporating the ac analysis on the violation index.

violation index is lower when ac line flows are integrated in the selection process. This suggests incorporating the ac analysis in GMD mitigation for improved performance. Note that in the second scenario with the ac flows included, the violation index increases significantly when the number of opened lines exceeds 14. The algorithm may be terminated at this point (no more lines are opened) if the user decides that the resulting violation index is unsatisfactory and the system security is compromised, i.e., the violation index can serve as a termination criterion to ensure system security.

The GIC-saturated loss in the individual transformers before and after utilizing the line switching algorithm is illustrated in Fig. 6. The algorithm reduces the losses significantly in most of the transformers. The losses remain unchanged or even slightly increased for few of the transformers. Developing techniques to restrict the losses in each transformer as opposed to the minimizing the overall loss will be an interesting future study.

C. A 2000-Bus Synthetic System

The last system to study is a 2000-bus synthetic system with the one-line diagram shown in Fig. 7 [29], [30]. The system has eight geographic areas which are color-coded in the one-line diagram; red lines are 345 kV and black lines are 115 kV.

An electric field with 8v/km magnitude and 91° N orientation (the direction with highest GICs) is enforced to the system. The

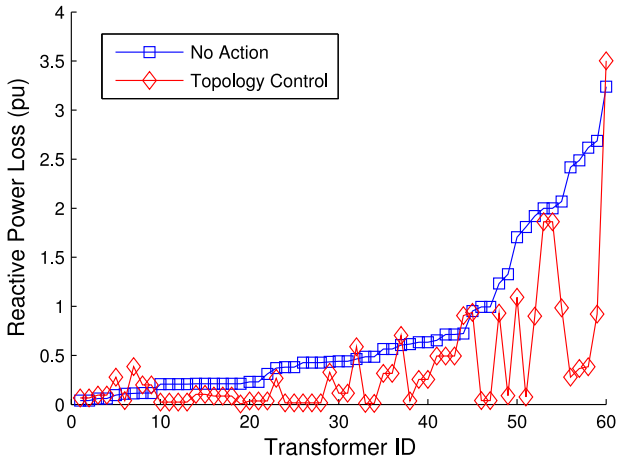

Fig. 6. GIC-saturated loss in the individual transformers before and after utilizing the topology control.

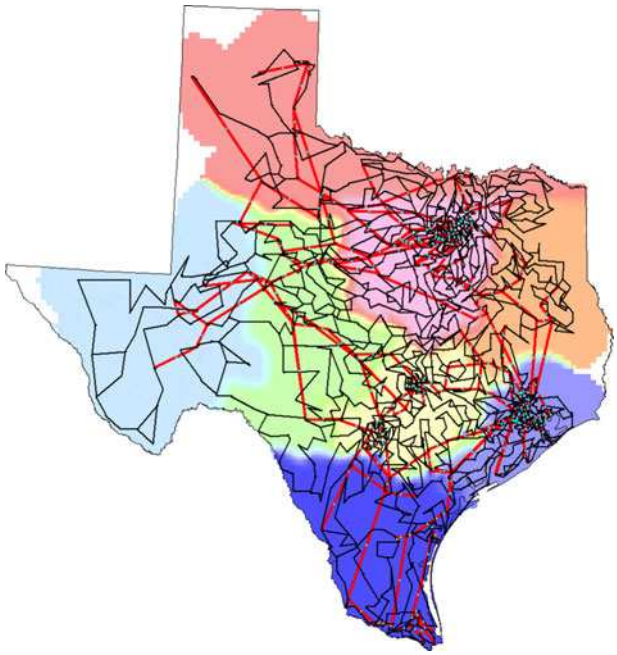

Fig. 7. One-line diagram of the 2000-bus synthetic system. (a) Eight geographic areas are color-coded. (b) Red lines are 345 kV and black lines are 115 kV.

GIC-saturated loss is calculated and the line selection algorithm is applied to find the best switching strategy. The system is large with 3024 lines and it is important to reduce the computational complexity using the technique presented in Section IV-A. Three scenarios are considered:

A) All the lines are considered and the full TLODF matrix is updated in each iteration.
B) 100 critical lines are selected and the full TLODF matrix is not updated ($C = 100$, U is not defined).
C) 100 critical lines are selected and the full TLODF matrix is updated after every 40 iterations ($C = 100$, $U = 40$).

Fig. 8 illustrates the total loss in terms of the number of opened lines for the three scenarios. AC analysis is not incorporated in this study and TLODFs are the only criteria for the line selection. It is assumed that maximum 80 lines can be opened (opening more lines deteriorates the system security as will be shown later on). It is observed that using constant TLODFs (scenario B) provides the same loss as updated TLODFs (Scenario A) when the number of opened lines is smaller than 40 and start to diverge afterwards. Hence, it is reasonable to recalculate the TLODFs and update the list of critical lines after each 40 iterations, i.e., $U = 40$ (scenario C).

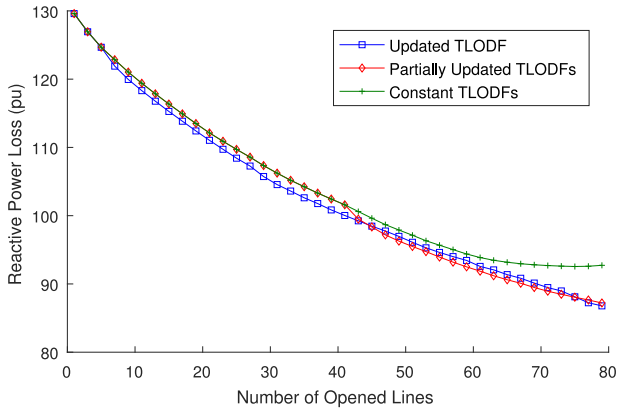

Fig. 8. Effect of the TLODF update frequency on the performance of the algorithm for the 2000-bus synthetic system.

TABLE III
ANALYZING THE COMPUTATIONAL COMPLEXITY OF THE ALGORITHM EXCLUDING THE AC ANALYSIS

Scenario	Running Time (s)	Total Loss (pu)	Running time Calculation
No Action	–	129.6	–
A) Updated TLODFs	851	87.23	$(L + ML)T$
B) Constant TLODFs	36.35	92.5	$(L + MC)T$
C) Partially Updated TLODFs (40 iteration)	56.32	86.87	$(2L + MC)T$
D) Exhaustive Search	4.7e + 156*	NA*	$\binom{L}{M}T$
$L = 3024$, $M = 80$, $C = 100$, $T \simeq 0.0035$ s			

∗ Exhaustive Search is not performed and the running time is estimated.

Table III presents the running time and the resulting GIC-saturated loss of the three scenarios. In this study, ac power flow is not solved in any of the iterations to reduce the running time and the bus voltages of the base case is used in (17) to calculated the GIC flows. Performance of the algorithm incorporating the ac analysis is presented later on. For reference, the estimated running time of the exhaustive search is also presented in the table. Note that the exhaustive search is not implementable on this large system as it requires iterating through $\binom{L}{M} = \binom{3024}{80} = 1.3613e + 159$ combinations of selecting 80 lines among 3024 lines. It is observed that the scenario with the partially updated TLODFs provides the same performance as the one with the updated TLODFs while its running time is much lower. This scenario is used in all the later studies throughout the paper due to its better performance.

Next, the AC analysis is incorporated into the algorithm as proposed in Section IV-B to ensure system security. Table IV presents the impact of incorporating ac analysis on the running time. Maximum opened lines is assumed to be 80. Recall that the selection criterion takes ac flows as input and the ac power

TABLE IV
ANALYZING THE COMPUTATIONAL COMPLEXITY OF THE ALGORITHM INCORPORATING THE AC ANALYSIS

Scenario	Running Time (s)	Total Loss (pu)
No Action	–	129.6
1) No AC Analysis	56.32	86.87
2) Updated AC Flows	181.31	95.16
3) Partially Updated ac Flows (8 Iterations)	72.47	91.14

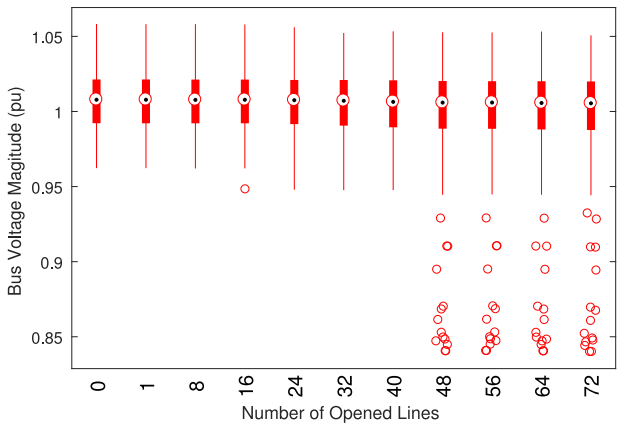

Fig. 9. Distribution of the bus voltage magnitudes at different steps of the algorithm when ac analysis is incorporated.

flow is solved at each iteration to update them. Updating the ac flows after several iterations as opposed to every single iteration can reduce the running time associated with solving power flow while still providing satisfactory performance (Third scenario in the table).

Incorporating the ac flows into the line selection improves the voltage profile and contributes to system security. Fig. 9 shows the box plot of the bus voltages depicting their maximum, minimum and the quartiles at different steps of the algorithm (the results for every eight iterations are presented in the figure for better clarity and conciseness). The circles in the figure are the suspected outliers whose values deviate from the quartiles by more than 150% of the interquantile range (IQR). It is observed that the bus voltages remain within the permissible range up to the 40th iteration. As more lines are opened, the voltage at some of the buses drops to 0.85 which may cause voltage instability.

Fig. 10 illustrates the advantage of using the ac line flows as part of the line selection criteria in maintaining the system security. The voltage violation index in (17) is calculated under two scenarios: 1) using TLODF as the selection criteria , 2) using the combination of TLODFs and ac line flows. The voltage security is maintained up to the 48th iteration when the ac line flows are incorporated whereas it starts to deteriorate at the 25th iteration without them. The algorithm may be terminated at the 25th iteration in the first scenario or the 48th iteration in the second scenario if the user decides that the violation index is unacceptable and the system security is compromised.

Next, the impact of the proposed line switching on the line MW flows is studied. Fig. 11 illustrates the maximum MW line

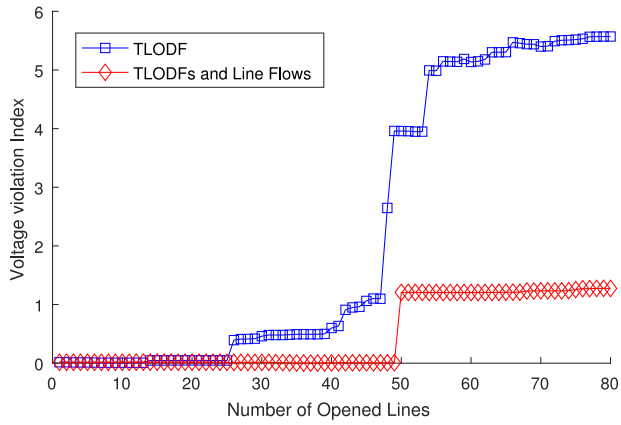

Fig. 10. The impact of incorporating the ac analysis on the voltage violation index.

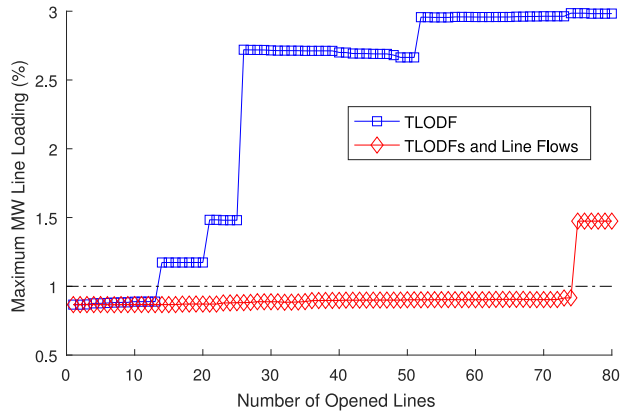

Fig. 11. The advantage of incorporating the ac flows in satisfying the line flow limits.

loadings (ratio of the MW flow to the MW limit) among all the lines in the network. All the line flows are below the limit when the ac flows are part of the selection criteria whereas the lines start to overload after the 11th iteration when only the TLODFs are considered in the selection process.

VI. CONCLUSIONS

In this paper, a novel line switching algorithm is developed to mitigate the negative impacts of GMDs. The algorithm minimizes the GIC-saturated reactive power loss based on TLODFs (counterparts of LODFs in GIC analysis). Some aspects of the ac analysis are considered to provide sufficient ac-related security measures. The computational complexity of the algorithm is analyzed and heuristics are utilized to reduce its running time for large-system applications. The algorithm performance is evaluated through numerical results using the small 20-bus system, the medium-size 150-bus synthetic case and the large 2000-bus system. The main observations are as follows:

1) Considering the ac line flows as an additional criterion for selecting the best lines improves the overall performance in terms of ac and dc power flow solutions.
2) The optimality of the proposed strategy was evaluated by comparing it with the exhaustive search in the small 20-bus system. The numerical results indicate that while the

algorithm does not find the optimal solution, it gets very close to it (finds the second best solution).

3) The heuristics used for fast computation are evaluated through case studies on the 2000-bus synthetic system. It was observed that that the running time of the proposed algorithm can be reduced significantly without compromising its performance.

The paper suggests several directions for future research. First, the proposed algorithm minimizes the total loss in the system, but does not impose any limit on the loss of individual transformers. The algorithm can be further refined to restrict the losses in each transformer while minimizing the total loss. Second, the proposed violation index serves as a final security check after the line switching is obtained, but does not provide any solution when the resulting security is unsatisfactory. Future research tends to address this by integrating the violation index into the line selection process to ensure voltage security of the resulting action. Last, this paper focuses on line switching as the remedial action. This framework can be extended to other types of actions such as shunt capacitor switching and neutral blocking devices in future research.

REFERENCES

[1] "2012 special reliability assessment interim report: Effects of geomagnetic disturbances on the bulk power system," North Amer. Electr. Rel. Corp., Atlanta, GA, USA, Tech. Rep., Feb. 2012.

[2] V. D. Albertson, J. M. Thorson, R. E. Clayton, and S. C. Tripathy, "Solar-induced-currents in power systems: Cause and effects," *IEEE Trans. Power App. Syst.*, vol. PAS-92, no. 2, pp. 471–477, Mar. 1973.

[3] D. H. Boteler and R. J. Pirjola, "Modelling geomagnetically induced currents produced by realistic and uniform electric fields," *IEEE Trans. Power Del.*, vol. 13, no. 4, pp. 1303–1308, Oct. 1998.

[4] T. J. Overbye, T. R. Hutchins, K. Shetye, J. Weber, and S. Dahman, "Integration of geomagnetic disturbance modeling into the power flow: A methodology for large-scale system studies," in *Proc. North Amer. Power Symp.*, Sep. 2012.

[5] "Executive order-coordinating efforts to prepare the nation for space weather events," White House Office of the Press Secretory, Washington, DC, USA. Tech. Rep., Apr. 2016.

[6] "FERC 830-reliability standard for transmission system planned performance for geomagnetic disturbance events," Federal Energy Regulatory Commission, Washington, DC, USA, Tech. Rep., Sep. 2016.

[7] J. Kappenman, "Low-frequency protection concepts for the electric power grid:Geomagnetically induced current (GIC) and E3 HEMP mitigation," Oak Ridge Nat. Lab., Oak Ridge, TN, USA, Tech. Rep., 2010.

[8] J. G. Kappenman *et al.*, "GIC mitigation: a neutral blocking/bypass device to prevent the flow of GIC in power systems," *IEEE Trans. Power Del.*, vol. 6, no. 3, pp. 1271–1281, Jul. 1991.

[9] H. Zhu and T. J. Overbye, "Blocking device placement for mitigating the effects of geomagnetically induced currents," *IEEE Trans. Power Syst.*, vol. 30, no. 4, pp. 2081–2089, Jul. 2015.

[10] E. Arajärvi, R. Pirjola, and A. Viljanen, "Effects of neutral point reactors and series capacitors on geomagnetically induced currents in a high-voltage electric power transmission system," *Space Weather*, vol. 9, no. 11, 2011.

[11] L. Bolduc, M. Granger, G. Pare, J. Saintonge, and L. Brophy, "Development of a dc current-blocking device for transformer neutrals," *IEEE Trans. Power Del.*, vol. 20, no. 1, pp. 163–168, Jan. 2005.

[12] B. Kovan and F. de León, "Mitigation of geomagnetically induced currents by neutral switching," *IEEE Trans. Power Del.*, vol. 30, no. 4, pp. 1999–2006, Aug. 2015.

[13] J. G. Kappenman, "Mitigation of geomagnetically induced and dc stray currents," Electr. Power Res. Inst., Palo Alto, CA, USA, Tech. Rep. EL-3295, 1983.

[14] A. A. Hussein and M. H. Ali, "Suppression of geomagnetic induced current using controlled ground resistance of transformer," *Electr. Power Syst. Res.*, vol. 140, pp. 9–19, 2016.

[15] J. G. Rolim and L. J. B. Machado, "A study of the use of corrective switching in transmission systems," *IEEE Trans. Power Syst.*, vol. 14, no. 1, pp. 336–341, Feb. 1999.

[16] W. Shao and V. Vittal, "Corrective switching algorithm for relieving overloads and voltage violations," *IEEE Trans. Power Syst.*, vol. 20, no. 4, pp. 1877–1885, Nov. 2005.

[17] K. Hedman, R. O'Neill, E. Fisher, and S. Oren, "Optimal transmission switching with contingency analysis," in *Proc. IEEE PES General Meeting*, Jul. 2010.

[18] E. A. Goldis, X. Li, M. C. Caramanis, A. M. Rudkevich, and P. A. Ruiz, "Ac-based topology control algorithms (TCA) – A PJM historical data case study," in *Proc. 2015 48th Hawaii Int. Conf. Syst. Sci.*, Jan. 2015, pp. 2516–2519.

[19] B. Gou and H. Zhang, "Fast real-time corrective control strategy for overload relief in bulk power systems," *IET Gener., Transmiss. Distrib.*, vol. 7, no. 12, pp. 1508–1515, Dec. 2013.

[20] A. A. Mazi, B. F. Wollenberg, and M. H. Hesse, "Corrective control of power system flows by line and bus-bar switching," *IEEE Power Eng. Rev.*, vol. PER-6, no. 8, pp. 53–53, Aug. 1986.

[21] M. Kazerooni, H. Zhu, K. Shetye, and T. J. Overbye, "Estimation of geoelectric field for validating geomagnetic disturbance modeling," in *Proc. Power Energy Conf. Illinois*, Feb. 2013, pp. 218–224.

[22] X. Dong, Y. Liu, and J. G. Kappenman, "Comparative analysis of exciting current harmonics and reactive power consumption from GIC saturated transformers," in *Proc. IEEE PES Winter Meeting*, Jan. 2001, pp. 318–322.

[23] T. J. Overbye, K. S. Shetye, T. R. Hutchins, Q. Qiu, and J. D. Weber, "Power grid sensitivity analysis of geomagnetically induced currents," *IEEE Trans. Power Syst.*, vol. 28, no. 4, pp. 4821–4828, Nov. 2013.

[24] T. Guler, G. Gross, and M. Liu, "Generalized line outage distribution factors," *IEEE Trans. Power Syst.*, vol. 22, no. 2, pp. 879–881, May 2007.

[25] F. L. Alvarado, "Computational complexity in power systems," *IEEE Trans. Power App. Syst.*, vol. PAS-95, no. 4, pp. 1028–1037, Jul. 1976.

[26] R. Yuster and U. Zwick, "Fast sparse matrix multiplication," *ACM Trans. Algorithms*, vol. 1, no. 1, pp. 2–13, Jul. 2005.

[27] R. Horton, D. Boteler, T. J. Overbye, R. Pirjola, and R. C. Dugan, "A test case for the calculation of geomagnetically induced currents," *IEEE Trans. Power Del.*, vol. 27, no. 4, pp. 2368–2373, Oct. 2012.

[28] A. B. Birchfield, K. M. Gegner, T. Xu, K. S. Shetye, and T. J. Overbye, "Statistical considerations in the creation of realistic synthetic power grids for geomagnetic disturbance studies," *IEEE Trans. Power Syst.*, vol. 32, no, 2, pp. 1502–1510, Mar. 2017.

[29] "Synthetic Power Cases-Illinois Center for a Smarter Electric Grid," [Online]. Available: http://icseg.iti.illinois.edu/

[30] A. B. Birchfield, T. Xu, K. M. Gegner, K. S. Shetye, and T. J. Overbye, "Grid structural characteristics as validation criteria for synthetic networks," *IEEE Trans. Power Syst.*, vol. 32, no. 4, pp. 3258–3265, Jul. 2017.

Maryam Kazerooni (S'11) received the B.S. degree in electrical engineering from the Sharif University of Technology, Tehran, Iran, and the M.S. degree in electrical engineering from the University of Windsor, Windsor, ON, Canada. She is currently working toward the Ph.D. degree in electrical engineering at the University of Illinois, Urbana, IL, USA. Her current research interests include power system reliability, state estimation, and geomagnetic disturbance analysis.

Hao Zhu (M'12) received the B.S. degree from Tsinghua University, Beijing, China, in 2006, and the M.Sc. and Ph.D. degrees from the University of Minnesota, Minneapolis, MN, USA, in 2009 and 2012, respectively. He is currently an Assistant Professor of ECE at the University of Illinois, Urbana, IL, USA. Her current research interests include power system monitoring and operations, dynamics and stability, and energy data analytics.

Thomas J. Overbye (S'87–M'92–SM'96–F'05) was born in Milwaukee, WI, USA. He received the B.S., M.S., and Ph.D. degrees in electrical engineering from the University of Wisconsin, Madison, WI, USA. He is currently the Fox Family Professor in the Department of Electrical and Computer Engineering at the University of Illinois, Urbana, IL, USA. His current research interests include power system visualization, power system dynamics, power system cyber security, and power system geomagnetic disturbance analysis.